Journal of the Korean Nuclear Society
Volume 11, Number 1, March, 1979

≪**Original**≫

Study of the Librational Motion of H_2O Molecules in Hydrates by Neutron Inelastic Scattering

Huhn-Jun Kim and Byung-Gook Yoon

Nuclear Physics Department
Korea Atomic Energy Research Institute, Seoul, Korea
(Recd. Nov. 25, 1978)

Abstract

Neutron inelastic scattering studies on polycrystalline hydrates, $NaBr \cdot 2H_2O$ and $BaCl_2 \cdot 2H_2O$ have been performed to observe librational modes. Assuming all observed peaks are from the H_2O librational origin, the weighted frequency distribution functions are obtained by eliminating the contributions from the higher order processes. All of theoretical frequencies obtained using FG matrix method are dus to highly mixed modes, and therefore the modes identified as significant H_2O librational modes from their large potential energy distributions are assigned to the observed peaks. The H—bond interactions are estimated using a modified Lippincott Schroeder potential function, and the applicability of the potential function to the H-bond with highly bent or bifurcated configuration is examined on the basis of the shape of H_2O librational potential energies. Some discussions are given on the usefulness of introducing O—H···Y bending terms in addition to the H···Y stretching in similar frequency calculation in order to obtain more information on the nature of H—bond. Also the purity and symmetry properties of the H_2O librational modes are discussed using group theoretical analyses.

요 약

수화물 결정에 있어서 H_2O 분자의 외부 각 운동을 조사하고저 $NaBr \cdot 2H_2O$ 및 $BaCl_2 \cdot 2H_2O$ 분말시료에 대한 중성자비탄성산란실험을 수행하였으며, 관측된 진동수를 모두 이 외부 각 운동에 의한 것으로 보고 다중 및 다준위산란효과를 제거하므로서 평균진동수 분포함수를 구하였다. FG 행열법에 의해서 계산된 진동수의 이론 값들은 모두 복합 mode에 의한 것이였으며 따라서 그 중 포텐샬·에네지분포가 큰 mode로서 관측치에 대한 assignment를 하였다. 소수결합력은 Lippincott-Schroeder 포텐샬함수에서 추산하였으며, 결선형 및 분기형수소결합에 대한 이 함수의 유용성을 H_2O 외부 각 운동 포텐샬함수 모양에 의거하여 검토하였다. 수소결합력의 성질에 대하여 더욱 자세한 자료를 얻기 위해서는 진동수 계산에 H···Y 신축상호작용 뿐만 아니라 O—H···Y 변각상호작용의 도입이 필요함을 논의하였고 또 H_2O 외부 각 운동에 있어서 mode의 순수성 및 대칭성을 군론을 적용한 방법에 의거하여 논의하였다.

1. Introduction

Neutrons are excellent probes to investigate the dynamics of hydrogenous compounds because

*This work was supported in part by the International Atomic Energy Agency, Vienna, Austria.

of the large incoherent cross-section of hydrogen. Measurements of neutron incoherent scattering spectra span modes of wide range of wavelengths (wave vector $|q|=10^{-3}$ to 1Å^{-1}), whereas the optical spectra are restricted to long wavelength modes only ($|q|\approx 0$). In addition, optical spectra are governed by certain selection rules. On the other hand, the neutron spectra, being free from constraints of such selection rules, exhibit all the modes in which hydrogen can take part. In neutron spectra, as a result, one may observe broad bands or even additional peaks due to large density of states at non-zero wave vector and the spectra, in fact, are related closely to the weighted frequency distribution function of the modes.

A number of inorganic hydrates have been investigated by neutron method to study the librational modes of H_2O molecules hydrogen-bonded in various crystalline environments[1,2,3,4]. The studies of this area are of wide interest in view of the facts, i) no definite assignment of the observed frequencies can be made easily except for some favourable cases[4,5] and, ii) very little is known quantitatively about the effects of hydrogen-bond (H-bond) interaction and metal-oxygen coordination involved on the dynamics of H_2O molecules, although it has been observed by several workers that the H-bond is dominant interaction to govern the H_2O librational motions in some hydrates.

In the present work, $NaBr\cdot 2H_2O$ (sodium bromide dihydrate, SBD) and $BaCl_2\cdot 2H_2O$ (barium chloride dihydrate, BCD) have been studied as representative examples of A- and B- type crystal water molecules in Chidambaram's classification[6]. The tetra-molecular unit cells of SBD and BCD belong to space group $P2_1/c$ and $P2_1/n$ respectively and have two types of crystallographically non-equivalent water molecules, H_2O(I) and H_2O(II). In the both hydrates, lone pairs of O atoms are approximately directed to metal ions and three of the four kinds of H atoms form approximately linear O—H···Y bonds, Y being the H-bond acceptors, Br or Cl ion. But in SBD H(2) is weakly bound in a highly bent H-bond whereas in BCD H(4) is loosely shared between two Cl ions forming a bifurcated H-bond. The relevant crystallographic data for these hydrates are summarized in Table 1[6,7].

Measurements were carried out using an inverted filter spectrometer with BeO as filter and the experimental remarks are described in Section 3. In section 4, the weighted frequency distribution function of the H_2O librational motions

Table 1. Geometry of Hydrogen-bonds and Oxygen Coordinates of Water Molecules in $NaBr\cdot 2H_2O$ and $BaCl_2\cdot 2H_2O$

	M—O (Å)	M—O—M (deg)	Type	O—H (Å)	H—O—H (deg)	O···Y (Å)	H···Y (Å)	O—H···Y (deg)	Y—O—Y (deg)
Na, O(1), H(1)···Br	2.48	101	A	0.99	104	3.37	2.38	177	81
Na, O(1), H(2)···Br	2.42			1.02		3.58	2.80	133	
Na, O(2), H(3)···Br	2.37	96	A	0.98	105	3.37	2.41	169	104
Na, O(2), H(4)···Br	2.41			1.01		3.32	2.32	167	
Ba, O(1), H(1)···Cl(2)	2.84	123	B	0.97	106	3.18	2.24	165	111
Ba, O(1), H(2)···Cl(2)	2.85			0.97		3.13	2.17	167	
Ba, O(2), H(3)···Cl(1)	2.87	117	B	0.97	103	3.18	2.22	171	
Ba, O(2), Cl(1)						3.30	2.66	125	
Ba, O(2), H(4)···Cl(2)	2.89			0.95		3.24	2.49	135	

are obtained from the observed spectra by eliminating contributions due to the higher order processes. The assignments of the observed peaks have been made by comparing with the theoretical frequencies calculated from FG matrix method in Section 5. For the estimation of the H-bond interactions between H_2O molecules and H-bond acceptors, we have resorted to a modified Lippincott-Schroeder potential function (LSPF). In order to look into the applicability of LSFF to the H-bond with highly bent or bifurcated configuration in some direct way, we have discussed the potential energies of H_2O librational modes on the basis of a simple model. Group theoretical analyses which provide informations on the purity and symmetry properties of the modes are also discussed here.

2. Experimental

The experiments were carried out at TRIGA Mark III reactor in Korea Atomic Energy Research Institute using an inverted filter spectrometer similar to those described in detail elsewhere[9,10]. Fig. 1 shows a schematic drawing of the experimental arrangement. Monoenergetic

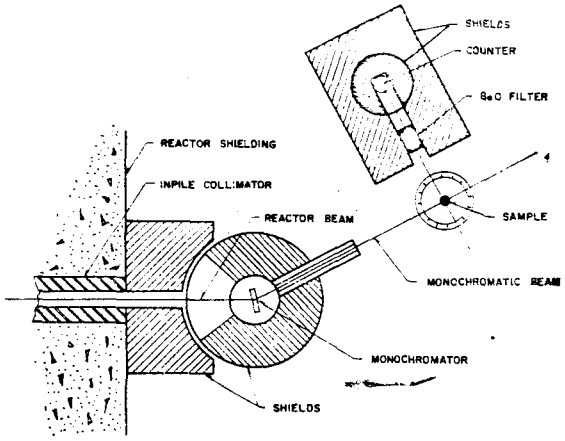

Fig. 1. Schematic view of the experimental arrangement (inverted filter spectrometer).

neutrons were selected from the pile spectrum by Bragg reflection using Cu(111) planes. These are then allowed to strike the sample and neutrons scattered therefrom were detected by a BF_3 counter placed vertically behind a 10 cm long polycrystalline BeO filter. The cross section of BeO is such that only those neutrons with energy less than 3.7 meV are transmitted and therefore the filter-detector combination acts an energy analyzer of constant window.

To observe the inelastic spectrum, the incident neutron energy was varied by changing the

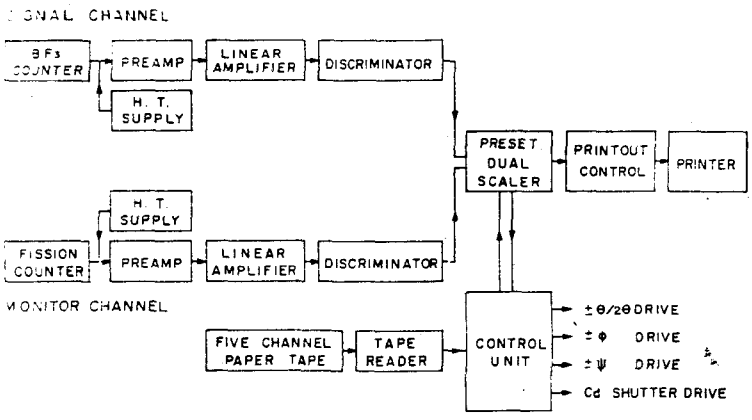

Fig. 2. Block diagram of counting and control electronics of the inverted filter spectrometer.

Bragg angle of the monochromator and the scattered neutron intensity at each position of the monochromator was recorded for a preset number of monitor counts of a thin fission counter placed on the incident beam. Discrete peaks associated with the various modes of motions in the system would be observed in the inelastic spectrum when the condition

$$E_0-\langle E_A\rangle\equiv\varepsilon=h\nu_i \qquad (1)$$

is satisfied; i. e. when the neutron after exciting i-th mode has just enough energy to get through the analyzer. Here E_0 is the incident neutron energy, ε is the energy transfer in the scattering process, ν_i is the frequency of the mode to which the neutron loses energy, and $\langle E_A\rangle=2.5$ meV is the average energy of BeO analyzer window.

The operation of the spectrometer is automatic. For a variety of experiments including the constant Q and E scans, the monochromator angle (θ_M), scattering angle (ϕ) and sample orientation (Ψ) can be changed nonlinearly by means of five channel paper tape on which instructions are perforated. For the present work with polycrystalline samples, ϕ was kept at 90° for all measurements and θ_M was changed in steps of 0.1°.

The samples were obtained by cooling aqueous solution in a sealed atmosphere. Similarly, deutrated sample of SBD. was prepared by dissolving the anhydrate in D_2O(99.89mole %) and cooling. As the compounds become readily dehydrated in vacuum, the powder forms of samples were packed in the air-tight aluminium container of 50 mm diameter and 0.75 mm wall thickness, and held in half-angle transmission geometry in the liquid nitrogen cryostat which has provision to vary the sample temperature by adjusting the electric current through a heater fastened around the sample container. The sample temperature was continuously monitored by two thermocouples attached to the top and bottom of the sample container and the temperature fluctuation was less than ±4°K throughout the experiment. The neutron transmission through the samples were about 70%.

3. Observation

Measurements were performed mainly over the H_2O librational frequency region and the results are summarized in Figs. 3 and 4 after correcting for the background. The error bars are based on counting statistics alone. In Fig. 3 all spectra are shown on the same intensity scale by normalizing measurements for the same monitor counts.

The SBD spectrum at 100°K shows three distinct peaks at 403, 562, 650 cm^{-1} and an indistinct peak around 474 cm^{-1} as shoulder.

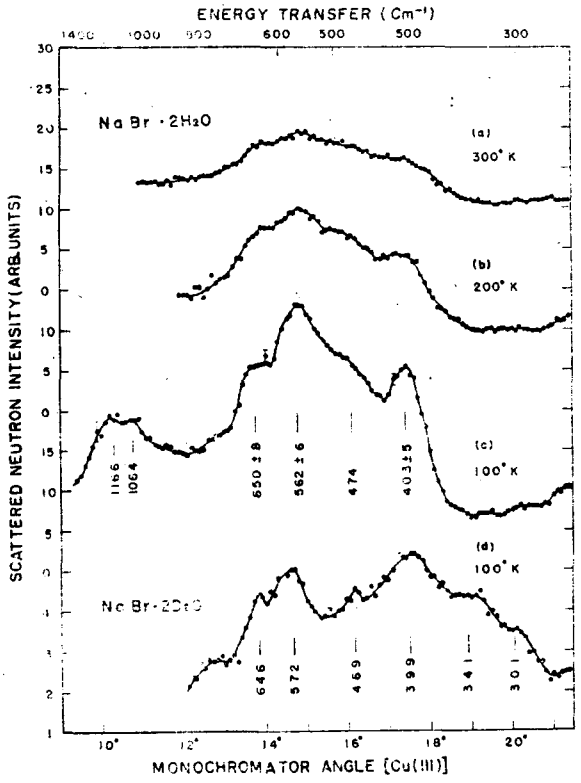

Fig. 3. The neutron inelastic scattering spectra of $NaBr\cdot2H_2O$ and $NaBr\cdot2D_2O$.

Two peaks at 1, 064 and 1, 166 cm^{-1} are considered mainly due to the multi-phonon process as discussed in detail in Section 4. With increasing temperature, rapid decrease of peak intensities are seen and RT data gives only a broad distribution barely showing the evidence of three peaks. As seen more clearly from 210°K spectrum, however, there is no remarkable change in the general feature of distribution and the position of peaks.

The NMR study of SBD showed a large drop of the second moment above 174°K and for the partial explanation of this Sarma[11] suggested a model in which H_2O(I) molecules excecute free rotation about the line joining the linear O—H···Br bond above the temperature. If H_2O molecules excecute rotation with frequency comparable with those of the librational modes, cne can expect that the peaks due to the librational modes will be all washed out in neutron inelastic spectrum[12,13]. Persistance of similar feature of spectrum up to RT, as seen in Fig. 3, therefore suggests that (i) H_2O molecules are excecuting reorientational motions with frequencies much lower than librational frequencies, and (ii) SBD does not undego any phase transition which could bring significant change of crystal structure and accordingly dynamics of H_2O molecules up to RT. The spectrum of the deutrate was obtained only for SBD to confirm the librational nature of peaks observed in the hydrate by isotopic shift. As compared in the same figure, all peaks are found to shift to lower frequencies with isotopic ratios of about $\sqrt{2}$. The intensities of two peaks which persist around 572 and 646 cm^{-1} could be due to about 2% of hydrate impurity.

For BCD the neutron time-of-flight spectrum at RT was reported by Boutin[1]. In the present work we have taken spectrum only at 100°K and four peaks at 423, 531, 601 and 717 cm^{-1} and an indistinct peak around 568 cm^{-1} are

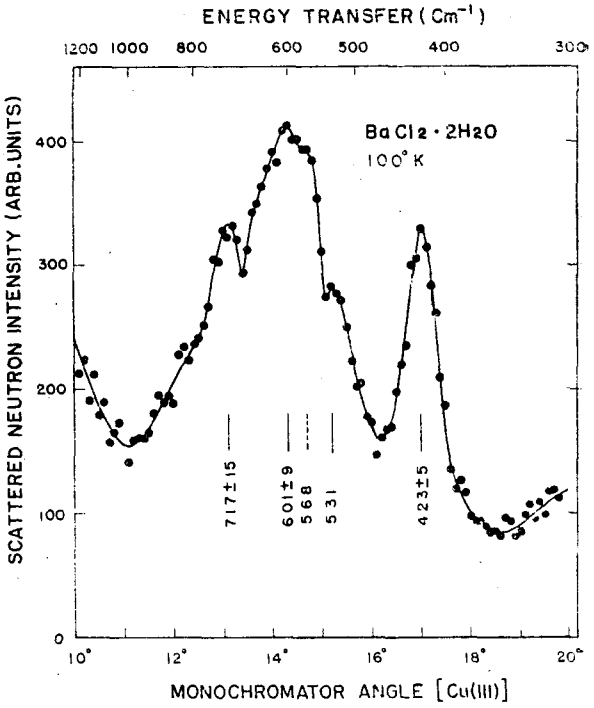

Fig. 4. The neutron inelastic scattering spectrum of $BaCl_2 \cdot 2H_2O$.

observed as seen in Fig. 4. The peaks observed in the present experiment are summarized in Table 10 along with earlier results obtained by neutron[1] and optical methods[14,15].

4. Weighted frequency distribution function of H_2O librational mode

The scattering of slow neutrons from hydrates are predominantly from proton and incoherent. Further, at low temperatures the inelastic scattering is almost entirely by the excitation or de-excitation of the external modes since the internal modes, which have large energies, can not be excited either thermally or by the neutrons. It is observed by several authors[3,16] that the frequency districution function can be extracted from the incoherent scattering data even for molecular solids in favourable cases. The main requirement for this is that the translational and

librational parts of the spectrum should be well seperated, and we assumed this is the case with the present samples in view of the fact that for a lage number of crystal hydrates the H_2O librational modes fall in 300~900 cm^{-1} range, while the translatory modes lie around or below 300 cm^{-1} [1,17].

The measured neutron spectrum includes invariably contributions from two kinds of higher order processes involving multiple number of phonon*. One is referred as 'multi-phonon' process and the other as 'multipul-scattering' process. In multi-phonon process, we are concerned with the neutron exchanging energy (gain or loss) with a single nucleus in the sample system due to zero phonon, one phonon, two phonon etc. processes. Multiple scattering refers to contributions arising from more than one scattering process in the sample system, that is at more than one scattering nucleus, in each scattering of which, multi-phonon processes are allowed. Clearly the multiple scattering process depend on the number of nuclei present in the sample and therefore on the size and shape of the sample,

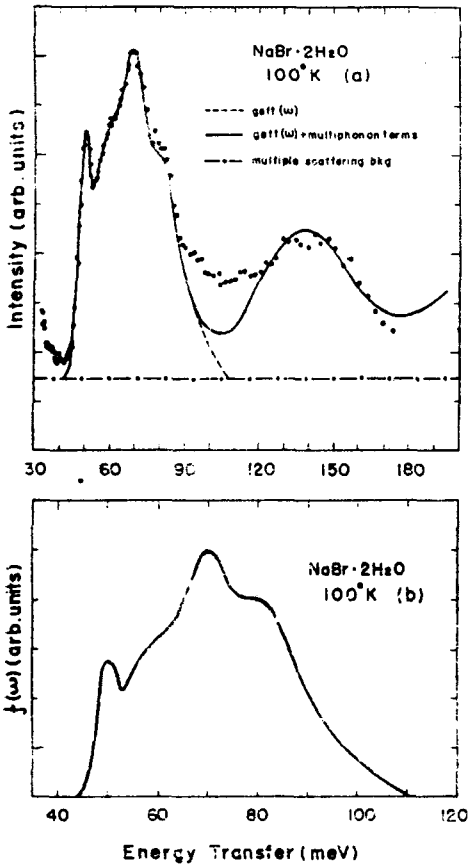

Fig. 5. (a) Spectrum from $NaBr \cdot 2H_2O$ is compared with the calculated cross-section, i.e., the effective librational spectrum, $g_{eff}(\omega)$, plus the contribution due to multi-phonon processes (see text). (b) Weighted frequency distribution function of H_2O librational modes, $f(\omega)$, calculated from $g_{eff}(\omega)$.

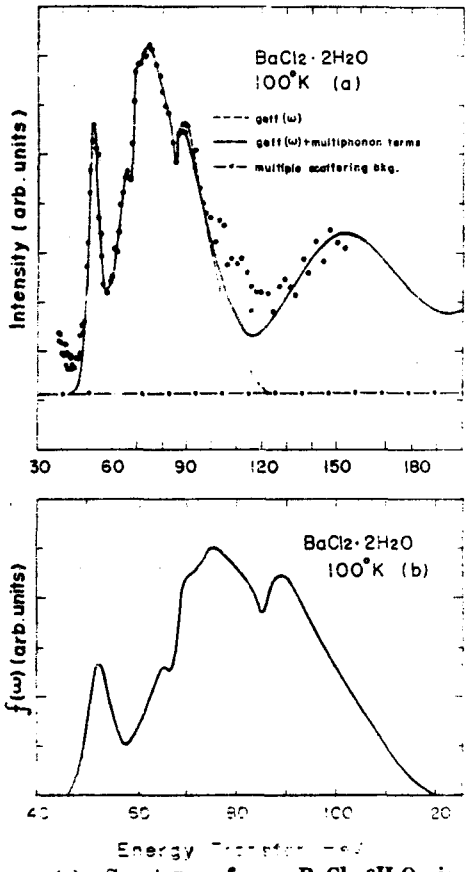

Fig. 6. (a) Spectrnm from $BaCl_2 \cdot 2H_2O$ is compared with the calculated cross-section, i.e., the effective librational spectrum, $g_{eff}(\omega)$, plus the contribution due to multi-phonon processes (see text). (b) Weighted frequency distribution function of H_2O librational modes, $f(\omega)$, calculated from $g_{eff}(\omega)$.

and many works were reported for the calculation of this contributon. With the inverted filter spectrometer, however, one has to consider the additional contribution arising from those neutrons which have energies greater than the filter cut-off energy but reach the detector after undergoing multiple or small angle scattering in the filter[18]. Because of the complication involved in the detailed theoretical shape analysis of this contribution, we simply assumed that those contributions due to multiple and small angle scattering in the filter and multiple scattering in the sample are fairly smooth over the entire energy transfer range for incoherent scattering, and the background which appeared over and above the room background as shown by broken lines in Figs. 5-a and 6-a were subtracted before applying the multi-phonon corrections.

To evluate corrections due to multi-phonon processes, we have adopted the scheme of Sjolander[19] as this is easily amenable to numerical computation. We briefly discuss the relevant equations;

The total incoherent scattering cross section is given by

$$\frac{d^2\sigma}{d\Omega\, d\omega}=\sum_j \frac{\sigma_{inc,j}}{4\pi}\ \frac{k}{k_0}e^{-2W_j} \times\sum_{n=0}^{\infty}\frac{(2W_j)^n}{n!}G_n(\omega-\omega_0) \quad (2)$$

where $\hbar\omega$ and $\hbar\omega_0$ are energies of scattered and incident neutrons,

$\sigma_{inc,j}$; the total incoherent scattering cross section of the j-th nucleus,

k and k_0; the scattered and incident neutron wave vector,

e^{-2W_j}; the Debye-Waller factor of the j-th nucleus.

$G_n(\omega-\omega_0)$ is defined by recursion relations;

$$G_0(\omega)=\delta(\omega)$$
$$G_1(\omega)=g(\omega)=g_{eff}(\omega)$$
$$G_2(\omega)=\int_{-\infty}^{\infty}g(\omega-\omega')G_1(\omega')\,d\omega' \quad (3)$$
$$\cdots\cdots\cdots\cdots$$
$$G_n(\omega)=\int_{-\infty}^{\infty}g(\omega-\omega')G_{n1}(\omega')\,d\omega'$$

Here, $g(\omega)$ is related to the effective freqvency distribution, $f(\omega)$, as follows;

$$g(\omega)=\frac{f(\omega)}{2W}\frac{1}{2}\left\{\coth\left(\frac{\hbar\omega}{2k_BT}\right)-1,\right\}, \quad |\omega|\le\omega_m$$
$$=0, \quad |\omega|>\omega_m \quad (4)$$

with $f(\omega)=f_T(\omega)+\frac{3M}{2M_R}f_R(\omega)$. (5)

Here, $f_T(\omega)$ and $f_R(\omega)$ are the respective translational and rotational frequency distribution function, M and M_R are the respective molecular and effective rotational mass and ω_m the maximum vibrating frequency.

We observe two facts; (i) that the recursion relation helps in easy evaluation of contributions due to higher order processes, given $g(\omega)$ and (ii) $g(\omega)$ is directly proportional to once corrected $d^2\sigma/d\Omega\, d\omega$ if higher order contribution is estimated intuitively. One can then evaluate the total $G(\omega)$ starting from this $g(\omega)$ and compare with experimental $d^2\sigma/d\Omega\, d\omega$. We have adopted this approach in the data analysis, neglecting the translational part in Eq. (5). However, the error involved in this simplification will not be considerable in view of the fact that the scattering due to the librational part is relatively enhanced by a large mass factor (3 $M/2M_R$) compared to the translational part.

The normalization of the related functions are as follows;

$$\int_{-\infty}^{\infty}g(\omega)\,d\omega=1 \text{ and } \int_{-\infty}^{\infty}G_n(\omega)\,d\omega=1,$$

whereas $\int_0^{\infty}f(\omega)\,d\omega=1$.

$g(\omega)$ is not even function and $g(-\omega)$ can be obtained from the relation $f(\omega)=f(-\omega)$ and

*In this discussion we use the term 'phonon' to denote both the translational and rotational excitation energy quanta.

Eq. (4). $2W$ is calculated as function of Q using $f(\omega)$ and the relation

$$2W=\frac{2m_H}{\hbar Q^2}\int_0^\infty \coth(\beta\omega)\frac{f(\omega)}{\omega}d\omega, \quad (6)$$

with $\beta=\frac{\hbar}{2k_BT}$, k_B being the boltzmann constant, T the temperature of scattering sample, m_H the mass of hydrogen atom.

To start with, $g_{eff}(\omega)$ was isolated intuitively from the spectrum, and this input spectrum was adjusted by trial and error so that the resulting total scatteing cross section which contains up to 6th higher order contributions could represent the observed spectrum reasonably, as shown the results in Figs. 5-a and 6-a with individual spectrum $g_{eff}(\omega)$ by dotted line and the total scattering cross section by full line. Although there are discrepancies between calculations and experimental data around 100~120 meV which may be due to lack of our knowledge of $g_{eff}(\omega)$ below 40 meV, we believe that the agreement between calculated and measured distribution is reasonable. The effective frequency distribution extracted in the manner described above is shown in Figs. 5-b and 6-b. It may be remarked that these distributions are only "weighted" frequency distributions and related the frequency density function of the hydrate through polarization vectors associated with the various modes of librations. Out of all salient peaks of the frequency distribution functions only 423 cm^{-1} peak in BCD can be isolated approximately and the width (HWFM)~40 cm^{-1} is found roughly to agree with instrumental resolution at the corresponding energy transfer, suggesting fairly small dispersion of the associated librational branch.

In the region of the librational frequencies the number of the second order neutrons in the incident beam was invariably less than 10% and no correction has been mode for this contamination.

5. Theoretical analysis and discussion

To understand the dynamical nature of the external molecular motion of H_2O molecules in hydrates, one has to carry out theoretical analysis of $g_{eff}(\omega)$. There are two aspects to this problem; (i) to associate the effective frequency spectrum with various kinds of hydrogenic motions and (ii) to calculate the frequency distribution given a certain force field in the solid and compare with $g_{eff}(\omega)$. The first aspect can be studied by group-theoretical techniques and the latter by numerical methods. Calculation of theoretical $g_{eff}(\omega)$ is quite a labourous problem. A better alternative is to calculate the eigenvalues and eigenvectors of the dynamical matrix starting from the force field if this is known and then make comparisons with frequencies and intensities of observed modes. Two approaches are possible using either the Born von Karman theory or Wilson FG matrix method. In both approaches there are two major difficulties namely (i) there is very little theoretical basis for choosing suitable force fields and (ii) there is no known general force field applicable to all cases even a'priori.

It has been observed for some hydrates[3,14] that the H_2O librational motions are primarily sensitive to H-bond interactions. In order to examine the nature of H-bond on the librational motion more conveniently, we have preferred to calculate the frequencies associated with the long-wave modes only using FG method and make a comparison with the observed frequencies. This approaches is supported partly by the fact that the dispersion of the librational branches of hydrates is generally not large due to weak H_2O—H_2O interactions.

For the H-bond interaction between H_2O molecule and the H-bond acceptors, we have adopted the Lippincott-Schroeder potential func-

tion (LSPF)[20] based on the semi-empirical model, and modified for non-linear configuration by Chidambaram and Sikka[21]. If H-bonds of H_2O molecules are of the longer and weaker type, as are the cases with the present samples, and if the librational amplitudes are not large, the H-bond P.E. in O—H···Y bond can be approximated by H···Y interaction alone;

$$U(\mathrm{H}\cdots\mathrm{Y}) = -CD \exp[-n(r-r_0)^2/Cr]. \quad (7)$$

Here D is the dissociation energy of the H—Y bond and r_0 is it's equilibrium seperation. r is interatomic distance of the H···Y bond and C is a factor which takes into account the weakness of the H···Y bond at the same seperation and the quantity n is related to the stretching force constant k_0 of the H—Y by the relation $n=k_0r_0/D$.

Before going into the theoretical analysis mentioned above, we have calculated the potential energies of tho H_2O librational modes and their frequencies derived therefrom on the basis of a simple model with a view to examining the nature of LSPF on the H-bond with highly bent or bifurcated configuration in some direct way.

(i) Simple model

In this approach, the H_2O molecule bounded into the crystal is assumed to be rigid and to have three independent librational modes about its three principal axes at its center of mass, viz, the wagging mode (about the A axis), the twisting mode (about the two-fold B axis) and the rocking mode (about the C axis perpendicular to the molecular plane). The potential for the librational motion of the H_2O molecule in each of the three modes has been calculated as a function of it's amplitude by assuming that all the rest of atoms in the crystal to be fixed at their equilibrium positions.

The contribution from the H-bond between H_2O molecule and H-bond acceptor atoms has been obtained from Eq. (7) using the constants as given in Table 2. The quantity n has been obtained from the respective stretching force constant of HBr and HCl, 4.12 md/Å and 5.16 md/Å. A constant $c=0.715$ was found by Lippincott and Schroeder to be suitable for all type of linear H-bonds and was also found to be satisfactory for non-linear O—H···O bonds by Chidambaram et al[21]. Hence this value is retained in the present calculation. The total energy of the bifurcated H-bond has been estimated by adding the constituent H···Y_1 and H···Y_2 interactions.

The contribution due to the electrostatic interaction of the H_2O molecule with the rest of the structure, excluding the H-bond acceptors,

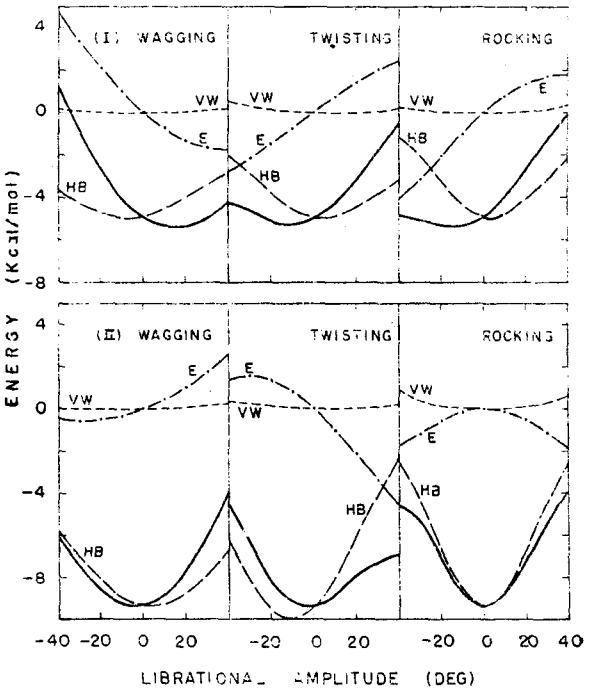

Fig. 7. Potential energy as a function of the libratienal amplitude of H_2O(I) and H_2O(II) in $NaBr\cdot 2H_2O$. E, electrostatic energy, VW, Van der Waals energy, HB, hydrogen-bond energy. The full line indicates the total energy.

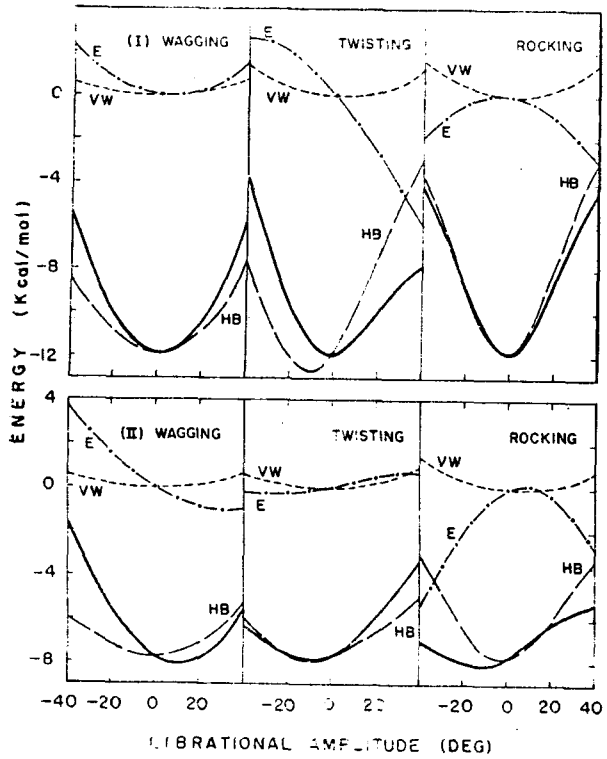

Fig. 8. Potental enery as a function of the librational amplitude of H_2O(I) and H_2O(II) in $BaCl_2 \cdot 2H_2O$. E, electrostatic energy, VW, Van der Waal's energy, HB, hydrogen-bond energy. The full lines indicate the total energy.

has been estimated by assigning formal point charges to various atoms. The interactions with interatomic distances of more than 24Å has been neglected. For the H_2O molecule the effective charges on atoms has been deduced from the dipole moment of water, 1.84(*D*). A value of unity has been used for the dielectric constant. Similarly, the Van der Waals energy has been estimated from Kitaigorodskii's formular[22] using the Van der Waals radii listed in Table 2.

The resulting individual and total potential energy curves of three librational modes for non-equivalent H_2O molecule are given in Figs. 7 and 8. For the H_2O molecule participated partly in highly bent or bifurcated configuration, much

Table 2. Constants used for the calculation of H-bond and non-bond potentials in the simple model.

	$NaBr \cdot 2H_2O$	$BaCl_2 \cdot 2H_2O$
Force Constant and Parameters involved in $U(H\cdots Y)$	$K(H-Br)=$ 4.12md/Å	$K(H-Cl)=$ 5.16md/Å
	$r_0=1.41$Å	$r_0=1.27$Å
	$D=86.7$ Kcal/mole	$D=103.2$ Kcal/mole
	$n=9.64$Å^{-1}	$n=9.14$Å^{-1}
	$C=0.715$	$C=0.715$
Charge(e)	Na : +1.0	Ba : +2.0
	Br : −1.0	Cl : −1.0
	H : +0.32	H : +0.32
	O : −0.64	O : −0.64
Dielectric Constant	1.0	1.0
Van der Waals radii (Å)	Na : 1.54	Ba : 2.16
	Br : 2.02	Cl : 1.75
	H : 1.20	H : 1.20
	O : 1.52	O : 1.52

weaker H-bond potential energies are seen. As seen in Table 1, H···Y distances are larger when they are involved in highly bent or bifurcated bond ranging from 2.49 to 2.80Å, compared with the cases of approximately linear bonds. For H_2O molecule in BCD, even the resulting energy of the bifurcated bond from H(4)···Cl(1) and H(4)···Cl(2) interactions is still weaker than that of H(3)···Cl(1) interaction, since the shorter the bond, the shaper is the increase in $U(H\cdots Y)$ of Eq. (7).

For H_2O molecules involved only in approximately linear bonds their total potential energy minima can be taken to represent the structural equilibrium positions satisfactory in the both samples, whereas for H_2O(I) in SBD and H_2O (II) in BCD these energy curves exhibit considerable assymmetric feature and their minima are deviated from the structural data*.

The potential due to the non-bond interactions of O atom have been negligible and the same

remained even when the effect of it's lone pair electrons has been taken into account by assuming the charge distribution according to Pople's model[23]. The librational frequencies estimated by fitting the harmonic potentials over the amplitude of $\pm 15°$[11] for total P. E. curves and also for P. E. curves due to the H-bond interaction alone are compared with the observed frequencies in Table 10.

(ii) Group theoretical analysis of dynamical modes of H_2O

The symmetry properties of normal modes of any crystal can be studied by using the formalism given by Maraudin and Vosko[24]. This method has been extended to external modes by Venkataraman et. al.[25]. One can study by these methods several aspects of "an arbitrary crystal belonging to an arbitrary symmorphic or non-symmorphic space group". The power of group-theoretical analysis can be used for this problem because it is possible to construct a set of matrices in the $3n$ dimensional space of eigenvectors corresponding to crystal symmetry operations, providing a matrix representation of the relevant group $G_0(q)$ of the wave-vector q. Without going into the details, it is sufficient for our purpose to mention the followings; If we restrict ourselves to those operations $R_m[=\{R|v(R)+x(m)\}]$ of the space group $G(q)$ of q, the purely rotational elements {R} in this space group, form a point group $G_0(q)$ called the group of the wave vector q. We can associate with each element R of $G_0(q)$ a matrix $T(q, R)$, whose elements are given by

$$T^{ii'}{}_{\alpha\beta}(k, k', q, R_m) = R_{\alpha\beta} C^i \delta_{ii'} \cdot \delta(k, F_0(k', R)) \exp\{iq[x(k) - Rx(k')]\}. \quad (8)$$

Here R_m is an element of $G(q)$, $R_{\alpha\beta}$ is the (α, β)th element in matrix representation R of the rotational part of R_m. i and i' comprehensively represent t and r signifying translation and rotation respectively. $C^i(R)$ is given by

$C^i(R) = 1$ if $i = t$
$= \det(R)$ if $i = r$;
$= 1$ for proper rotations
$= -1$ for improper rotaions

Table 3. Atomic interchanges by space group operations $P2_1/m(C^5_{2h})$ in $BaCl_2 \cdot 2H_2O$. Atoms in the molecular unit $BaCl_2 \cdot 2H_2O$ are labelled by number 1 to 9.

Mol/Atom	E mol/atom	C_2 mol/atom	i mol/atom	σ_h mol/atom
1 1	1 1	2 1	3 1	4 1
2	2	2	2	2
3	3	3	3	3
4	4	4	4	4
5	5	5	5	5
6	6	6	6	6
7	7	7	7	7
8	8	8	8	8
9	9	9	9	9
2 1	2 1	1 1	4 1	3 1
2	2	2	2	2
3	3	3	3	3
4	4	4	4	4
5	5	5	5	5
6	6	6	6	6
7	7	7	7	7
8	8	8	8	8
9	9	9	9	9
3 1	3 1	4 1	1 1	2 1
2	2	2	2	2
3	3	3	3	3
4	4	4	4	4
5	5	5	5	5
6	6	6	6	6
7	7	7	7	7
8	8	8	8	8
9	9	9	9	9
4 1	4 1	3 1	2 1	3 1
2	2	2	2	2
3	3	3	3	3
4	4	4	4	4
5	5	5	5	5
6	6	6	6	6
7	7	7	7	7
8	8	8	8	8
9	9	9	9	9

*For H_2O(I) in SBD, there are considerable differences between hydrogen positions located by Van Meerssche et al. using PMR method and by Ladd using crystal energy calculation. In the present work, the structural data from the former has been adopted since total potential energy curves obtained therefrom showed somewhat more favourable shapes.

Table 4. $T(0,R)$ matrices in $BaCl_2 \cdot 2H_2O$

$$T(0,E)=\begin{vmatrix} A & 0 & 0 & 0 \\ 0 & A & 0 & 0 \\ 0 & 0 & A & 0 \\ 0 & 0 & 0 & A \end{vmatrix} \qquad T(0,C_2)=\begin{vmatrix} 0 & B & 0 & 0 \\ B & 0 & 0 & 0 \\ 0 & 0 & B & 0 \\ 0 & 0 & 0 & B \end{vmatrix}$$

$$T(0,i)=\begin{vmatrix} 0 & 0 & C & 0 \\ 0 & 0 & 0 & C \\ C & 0 & 0 & 0 \\ 0 & C & 0 & 0 \end{vmatrix} \qquad T(0,\sigma_h)=\begin{vmatrix} 0 & 0 & 0 & D \\ 0 & 0 & D & 0 \\ 0 & D & 0 & 0 \\ D & 0 & 0 & 0 \end{vmatrix}$$

where 0 is a 21×21 null matrix. A, B, C and D are given by,

(i) in the atomic model

$$A=\begin{vmatrix} R_1 & 0 & 0 & 0 & 0 & 0 & 0 & 0 & 0 \\ 0 & R_1 & 0 & 0 & 0 & 0 & 0 & 0 & 0 \\ 0 & 0 & R_1 & 0 & 0 & 0 & 0 & 0 & 0 \\ 0 & 0 & 0 & R_1 & 0 & 0 & 0 & 0 & 0 \\ 0 & 0 & 0 & 0 & R_1 & 0 & 0 & 0 & 0 \\ 0 & 0 & 0 & 0 & 0 & R_1 & 0 & 0 & 0 \\ 0 & 0 & 0 & 0 & 0 & 0 & R_1 & 0 & 0 \\ 0 & 0 & 0 & 0 & 0 & 0 & 0 & R_1 & 0 \\ 0 & 0 & 0 & 0 & 0 & 0 & 0 & 0 & R_1 \end{vmatrix} \qquad B=\begin{vmatrix} R_2 & 0 & 0 & 0 & 0 & 0 & 0 & 0 & 0 \\ 0 & R_2 & 0 & 0 & 0 & 0 & 0 & 0 & 0 \\ 0 & 0 & R_2 & 0 & 0 & 0 & 0 & 0 & 0 \\ 0 & 0 & 0 & R_2 & 0 & 0 & 0 & 0 & 0 \\ 0 & 0 & 0 & 0 & R_2 & 0 & 0 & 0 & 0 \\ 0 & 0 & 0 & 0 & 0 & R_2 & 0 & 0 & 0 \\ 0 & 0 & 0 & 0 & 0 & 0 & R_2 & 0 & 0 \\ 0 & 0 & 0 & 0 & 0 & 0 & 0 & R_2 & 0 \\ 0 & 0 & 0 & 0 & 0 & 0 & 0 & 0 & R_2 \end{vmatrix}$$

$$C=\begin{vmatrix} R_3 & 0 & 0 & 0 & 0 & 0 & 0 & 0 & 0 \\ 0 & R_3 & 0 & 0 & 0 & 0 & 0 & 0 & 0 \\ 0 & 0 & R_3 & 0 & 0 & 0 & 0 & 0 & 0 \\ 0 & 0 & 0 & R_3 & 0 & 0 & 0 & 0 & 0 \\ 0 & 0 & 0 & 0 & R_3 & 0 & 0 & 0 & 0 \\ 0 & 0 & 0 & 0 & 0 & R_3 & 0 & 0 & 0 \\ 0 & 0 & 0 & 0 & 0 & 0 & R_3 & 0 & 0 \\ 0 & 0 & 0 & 0 & 0 & 0 & 0 & R_3 & 0 \\ 0 & 0 & 0 & 0 & 0 & 0 & 0 & 0 & R_3 \end{vmatrix} \qquad D=\begin{vmatrix} R_4 & 0 & 0 & 0 & 0 & 0 & 0 & 0 & 0 \\ 0 & R_4 & 0 & 0 & 0 & 0 & 0 & 0 & 0 \\ 0 & 0 & R_4 & 0 & 0 & 0 & 0 & 0 & 0 \\ 0 & 0 & 0 & R_4 & 0 & 0 & 0 & 0 & 0 \\ 0 & 0 & 0 & 0 & R_4 & 0 & 0 & 0 & 0 \\ 0 & 0 & 0 & 0 & 0 & R_4 & 0 & 0 & 0 \\ 0 & 0 & 0 & 0 & 0 & 0 & R_4 & 0 & 0 \\ 0 & 0 & 0 & 0 & 0 & 0 & 0 & R_4 & 0 \\ 0 & 0 & 0 & 0 & 0 & 0 & 0 & 0 & R_4 \end{vmatrix}$$

(ii) in the molecular model where we treat the water molecules as rigid units the $T(0,R)$ matrices have translational and rotational components due to corresponding degrees of freedom of the water molecule. A, B, C and D are given by

$$A=\begin{vmatrix} R_1 & 0 & 0 & 0 & 0 & 0 & 0 \\ 0 & R_1 & 0 & 0 & 0 & 0 & 0 \\ 0 & 0 & R_1 & 0 & 0 & 0 & 0 \\ 0 & 0 & 0 & R_1 & 0 & 0 & 0 \\ 0 & 0 & 0 & 0 & R_1 & 0 & 0 \\ 0 & 0 & 0 & 0 & 0 & R_1 & 0 \\ 0 & 0 & 0 & 0 & 0 & 0 & R_1 \end{vmatrix} \qquad B=\begin{vmatrix} R_2 & 0 & 0 & 0 & 0 & 0 & 0 \\ 0 & R_2 & 0 & 0 & 0 & 0 & 0 \\ 0 & 0 & R_2 & 0 & 0 & 0 & 0 \\ 0 & 0 & 0 & R_2 & 0 & 0 & 0 \\ 0 & 0 & 0 & 0 & -R_2 & 0 & 0 \\ 0 & 0 & 0 & 0 & 0 & R_2 & 0 \\ 0 & 0 & 0 & 0 & 0 & 0 & -R_2 \end{vmatrix}$$

$$C=\begin{vmatrix} R_3 & 0 & 0 & 0 & 0 & 0 & 0 \\ 0 & R_3 & 0 & 0 & 0 & 0 & 0 \\ 0 & 0 & R_3 & 0 & 0 & 0 & 0 \\ 0 & 0 & 0 & R_3 & 0 & 0 & 0 \\ 0 & 0 & 0 & 0 & -R_3 & 0 & 0 \\ 0 & 0 & 0 & 0 & 0 & R_3 & 0 \\ 0 & 0 & 0 & 0 & 0 & 0 & -R_3 \end{vmatrix} \qquad D=\begin{vmatrix} R_4 & 0 & 0 & 0 & 0 & 0 & 0 \\ 0 & R_4 & 0 & 0 & 0 & 0 & 0 \\ 0 & 0 & R_4 & 0 & 0 & 0 & 0 \\ 0 & 0 & 0 & R_4 & 0 & 0 & 0 \\ 0 & 0 & 0 & 0 & R_4 & 0 & 0 \\ 0 & 0 & 0 & 0 & 0 & R_4 & 0 \\ 0 & 0 & 0 & 0 & 0 & 0 & R_4 \end{vmatrix}$$

with

$$R_1=\begin{vmatrix}1&0&0\\0&1&0\\0&0&1\end{vmatrix}\quad R_1=\begin{vmatrix}1&0&0\\0&-1&0\\0&0&1\end{vmatrix}\quad R_3=\begin{vmatrix}-1&0&0\\0&-1&0\\0&0&-1\end{vmatrix}\quad R_4=\begin{vmatrix}-1&0&0\\0&1&0\\0&0&-1\end{vmatrix}$$

Table 5. Irreducible Representation for $G_0(0)$ in $BaCl_2 \cdot 2H_2O$

Repn.	Operations E	C_2	i	σ_h
A_g	1	1	1	1
A_u	1	1	−1	−1
B_g	1	−1	−1	1
B_u	1	−1	1	−1

Table 6. Symmetry Adopted Eigenvector Matrix for q=0 in $BaCl_2 \cdot 2H_2O$

$$\tilde{U}=\begin{vmatrix}A&A&A&A\\B&-B&B&-B\\C&-C&-C&C\\D&D&-D&-D\end{vmatrix}$$

A, B, C, D are defined in Table 4-(i)

The δ-function, $\delta(k, F_0(k', R))$ referring to interchange of sublattices if any, varnishes unless k corresponds to $F_0(k', R)$ arrived at from the sublattice k' via R_n in which case the delta function is unity. $x(k)$ and $x(k')$ are coordinates of the sublattices k and k'. k and k' can be atomic or molecular units. If there are μ atoms and η 'molecules' in the unit cell, $T(q, R)[R \in G_0(q)]$ provides a $(3\mu+6\eta)$ dimensional multiplier representation of $G_0(q)$. One can use the $T(q, R)$ matrices to classify the eigenvalues and eigenvectors by using the reduction formular,

$$C_s=\frac{1}{h}\sum_{R\in G_0(q)}\chi^s(q, R)^*\chi(q, R) \qquad (9)$$

where $\chi^s(q, R)$ and $\chi(q, R)$ are the characters of the irreducible and redubible multiplier representations of $G_0(q)$, h its order. C_s indicate the number of times the irreducible multiplier representation (IMR) $\tau^s(q)$ of dimensionality f_s occurs in the set $T(q, R)$. Correspondingly, there will be C_s eigenvalues each of which will be f_s-hold degenerate. The corresponding eigenvectors each can be labelled as

$$\{e(q, s, 1, 1)\cdots e(q, s, 1, f_s)\},$$
$$\{e(q, s, 2, 1)\cdots e(q, s, 2, f_s)\},$$
$$\cdots\{e(q, s, C_s, 1)\cdots e(q, s, C_s, f_s)\}.$$

One can project out C_s orthogonal symmetry adopted vectors

$$\xi(q, s, 1, \lambda)\cdots\xi(q, s, C_s, \lambda)$$

by using projection-operator technique. The eigenvectors $e(q, s, a, \lambda)$ are linear combination of $\xi(q, s, b, \lambda)$. The purity of the modes is decided by this linear combination. If $\xi(q, s, b, \lambda)$ is unique, $e(q, s, a, \lambda)$ is unique and hence the associated mode is pure and not otherwise.

In the following relevant representations and discussions are given for BCD Table 3 indicates interchange of sublattices as a result of space group operations. If we consider long wave modes only ($q=0$), the exponent $q\cdot(x(k)-x(k'))$ is zero. One can easily write down the $T(q, R)$ matrices. They are given in Table 4. At $q=0$, the IMR are the same as the irreducible representation for $G_0(0)$ which is given in Table 5. Table 6 gives the symmetry adopted eigenvectors belonging to various representations. An inspection of Table 6 is quite informative; The eigenvectors being linear combination of symmetry adopted vectors, we conclude the following from the table;

i) the rotational modes *can* all be mixed in character and there need not be purely rocking or wagging or twisting modes,

ii) the two H_2O molecules in $BaCl_2\cdot 2H_2O$ unit possess in-phase motion always,

iii) H_2O molecules in different $BaCl_2\cdot 2H_2O$ units can have in-phase and out-phase motion,

iv) the coherence effects due to ii) and iii) can affect the spectra in a deutrated sample, whereas this has no relevance in hydrogenous

Table 7. Summary of Factor Group Analysis of $BaCl_2 \cdot 2H_2O$

Representation	E	C_2	i	σ_h	Total	Acoustic	Trans. opt	Rotatory	External	Internal	
A_g	1	1	1	1	27	0	15	6	21	6	Raman
A_u	1	1	−1	−1	27	1	14	6	21	6	IR
B_g	1	−1	−1	1	27	2	13	6	21	6	IR
B_u	1	−1	1	−1	27	0	15	6	21	6	Raman
Total $\chi(n)$	108	0	0	0	$N_R(\pm 1+2\cos\theta)$						
Acoustic χ_A	3	−1	1	−3	$\pm 1+2\cos\theta$						
Optic trans χ_{op}	57	1	−1	3	$(N_R(s)-1)(\pm 1+2\cos\theta)$						
Rotational χ_R	24	0	0	0	$(N_R(s-m))\chi(p)$						

Notes: N_R; No. of atoms remaining invariant under point group operation R.
$N_R(s)$; No. of structural groups left in variant by R.
$N_R(s-m)$; No. of poly-atomic groups remaining invariant under R.
+ and − for proper and improper operations respectively.
$\chi(P)=1+2\cos\theta$ for nonlinear molecules, $=+2\cos\theta$ for linear except for C_h and σ_v.

compounds due to the preponderant incoherent cross section of hydrogen.

Before we conclude this section, for the sake of completeness we have given the results of factor group analysis of $BaCl_2 \cdot 2H_2O$ in Table 7. This analysis is useful in classifying the external modes into various categories of translational and rotational modes in infrared and Ramanactivities

(iii) FG method

For the optically active lattice vibrations the motion of all the Bravais cells take place in phase, and the F and G matrices for lattice vibrations are obtained by adding F and G matrices for one Bravais lattice (i. e., the smallest unit in which no two groups of atoms become equivalent as the result of a simple translation) to the sum of all matrices representing interactions between that Bravais cell and its neighbours. The matrices may be set up in terms of either internal or Cartesian coordinates. The treatment given below is essentially same as the Shimanouchi and Fukushima et. al'. s[26,27] approach but with Cartesian coordinates.

Let the matrices relating to optically active vibrations be G_{opt} and F_{opt}. If the Bravais cell is denoted by (i, j, k), we have

$$G_{opt}=N\sum_{i'j'k'} G_{(i,j,k;i'j'k')} \tag{10}$$

$$F_{opt}=N\sum_{i'j'k'} F_{(i,j,k;i'j'k')} \tag{11}$$

where N is normalization factor. It is possible to determine G_{opt} elements more readily by using Cartesian rather than internal coordinates, since G_{opt} is diagonal in Cartesian coordinates,

$$G_{opt(c)}=G_{(c)(i,j,k;i',j',k')} \tag{12}$$

its elements being the reciprocal masses of the atoms in the Bravais cell.

$F_{opt(c)}$ is related to F_{opt} as follows. There is a transformation matrix B such that R=BX where R and X are internal and Cartesian coordinates respectively. Then

$$F_{opt(c)}=\tilde{B}_{opt}F_{opt}B_{opt}. \tag{13}$$

Analogous to $R_{opt}=N\Sigma R_{(i,j,k)}$ in internal coordinates, we can define $X_{opt}=N\Sigma X_{(i,j,k)}$ as the Cartesian coordinates, representing X optically active vibrations. Then

$$B_{opt}=\sum_{i'j'k'} B_{(i,j,k;\ i',j',k')}. \tag{14}$$

This can also put as,

$$B_{opt}=\sum_{ijk} B_{(i,j,k;i',j',k')}. \tag{15}$$

The matrix elements B_{opt} are calculated only for the internal coordinates in terms of which the potential energy of the crystal is calculated.

Table 8. Interactions and force constants taken into account in the potential of the first molecular unit ($NaBr \cdot 2H_2O$)[1]. The Bravais cells of the interacting pair are indicated in reference to the atom (or ion) of the first molecular unit located in (i, j, k) cell.

	Interaction		Distance Å	Distance Å	Force Const. (md/Å)
R 1	(i,j,k) $(i-1,j,k)$	Na · · · O(1)	2.419		0.21
R 2	(i,j,k) $(i-1,j,k)$	Na · · · O(1)	2.482		0.19
R 3	(i,j,k) $(i,j-1,k)$	Na · · · O(2)	2.372		0.22
R 4	(i,j,k) (i,j,k)	Na · · · O(2)	2.405		0.21
R 5	(i,j,k) $(i-1,j,k)$	Br · · · O(1)	3,810		0.05
R 6	(i,j,k) (i,j,k)	Br · · · O(1)	3.910		0.05
R 7	(i,j,k) $(i+1,j-1,k)$	Br · · · O(1)	3.366		0.08
R 8	(i,j,k) (i,j,k)	Br · · · O(1)	3.576		0.07
R 9	(i,j,k) $(i-1,j,k-1)$	Br · · · O(1)	3.887		0.05
R10	(i,j,k) (i,j,k)	Br · · · O(2)	3.912		0.05
R11	(i,j,k) $(i,j-1,k)$	Br · · · O(2)	3.814		0.05
R12	(i,j,k) $(i+1,j-1,k)$	Br · · · O(2)	3.319		0.08
R13	(i,j,k) (i,j,k)	Br · · · O(2)	3.860		0.05
R14	(i,j,k) $(i,j,k-1)$	Br · · · O(2)	3.370		0.08
R15	(i,j,k) $(i,j,k+1)$	Na · · · Na	3.552		0.10
R16	(i,j,k) (i,j,k)	Na · · · Na	3.794		0.08
R17	(i,j,k) $(i,j,k-1)$	Na · · · Na	3.794		0.08
R18	(i,j,k) (i,j,k)	Na · · · Br	2.982		0.17
R19	(i,j,k) (i,j,k)	Na · · · Br	2.955		0.18
R20	(i,j,k) $(i+1,j,k)$	H(1) · · Br	2.380		0.63
R21	(i,j,k) $(i,j,k-1)$	H(2) · · Br	2.797		0.11
R22	(i,j,k) (i,j,k)	H(3) · · Br	2.406		0.58
R23	(i,j,k) $(i+1,j,k)$	H(4) · · Br	2,323		0.78
R24	(i,j,k) (i,j,k)	H(1)—O(1)	0.979		5.85
R25	(i,j,k) (i,j,k)	H(2)—O(1)	1.022		5.85
R26	(i,j,k) (i,j,k)	H(3)—O(2)	0.977		5.85
R27	(i,j,k) (i,j,k)	H(4)—O(2)	1.013		5.85
R28	$(i+1,j,k)$ (i,j,k) $(i+1,j,k-1)$	Na—O(1)—Na	2.419	2.482	0.04
R29	$(i+1,j,k)$ (i,j,k) (i,j,k)	Na—O(1)—H(1)	2.419	0.988	0.048
R30	$(i+1,j,k)$ (i,j,k) (i,j,k)	Na—O(1)—H(2)	2.419	1.022	0.048
R31	$(i+1,j,k-1)$ (i,j,k) (i,j,k)	Na—O(1)—H(1)	2.482	0.988	0.048
R32	$(i+1,j,k-1)$ (i,j,k) (i,j,k)	Na—O(1)—H(2)	2.482	1.022	0.044
R33	(i,j,k) (i,j,k) (i,j,k)	H(1)—O(1)—H(2)	0.988	1.022	0.750
R34	(i,j,k) (i,j,k) $(i,j,k-1)$	Na—O(2)—Na	2.372	2.405	0.05
R35	(i,j,k) (i,j,k) (i,j,k)	Na—O(2)—H(3)	2.372	0.977	0.06
R36	(i,j,k) (i,j,k) (i,j,k)	Na—O(2)—H(4)	2.372	1.013	0.06
R37	$(i,j,k-1)$ (i,j,k) (i,j,k)	Na—O(2)—H(3)	2.405	0.977	0.06
R38	$(i,j,k-1)$ (i,j,k) (i,j,k)	Na—O(2)—H(4)	2.405	1.013	0.06
R39	(i,j,k) (i,j,k) (i,j,k)	H(3)—O(2)—H(4)	0.977	1.013	0.75

Table 9. Interactions and force constants taken into account in the potential of the first molecular unit ($BaCl_2 \cdot 2H_2O$)[1]. The Bravais cells of the interacting pair are indicated in reference to the atom (or ion) of the first molecular unit located in (i,j,k) cell.

Interaction			Distance Å	Distance Å	Force Const. (mb/Å)
R 1	(i,j,k) $(i,j,k-1)$	Ba · · · O(1)	2.841		0.26
R 2	(i,j,k) $(i-1,j,k-1)$	Ba · · · O(1)	2.851		0.26
R 3	(i,j,k) (i,j,k)	Ba · · · O(2)	2.865		0.25
R 4	(i,j,k) $(i-1,j,k-1)$	Ba · · · O(2)	2.894		0.25
R 5	(i,j,k) $(i-1,j,k-1)$	Ba · · · Cl(1)	3.132		0.20
R 6	(i,j,k) $(i-1,j,k-1)$	Ba · · · Cl(1)	3.249		0.20
R 7	(i,j,k) $(i+1,j,k+1)$	Ba · · · Cl(1)	3.324		0.20
R 8	(i,j,k) $(i-1,j,k)$	Ba · · · Cl(2)	3.168		0.20
R 9	(i,j,k) $(i-1,j,k-1)$	Ba · · · Cl(2)	3.211		0.20
R10	(i,j,k) $(i+1,j,k)$	Cl(1) · · O(1)	3.665		0.04
R11	(i,j,k) (i,j,k)	Cl(1) · · O(1)	3.508		0.06
R12	(i,j,k) $(i+1,j,k+2)$	Cl(1) · · O(1)	3.477		0.07
R13	(i,j,k) $(i+1,j,k)$	Cl(1) · · O(2)	3.179		0.15
R14	(i,j,k) (i,j,k)	Cl(1) · · O(2)	3.493		0.06
R15	(i,j,k) $(i+1,j,k+1)$	Cl(1) · · O(2)	3.302		0.11
R16	(i,j,k) $(i,j,k-1)$	Cl(2) · · O(1)	3.130		0.17
R17	(i,j,k) $(i,j,k-1)$	Cl(2) · · O(1)	3.330		0.10
R18	(i,j,k) $(i+1,j,k+1)$	Cl(2) · · O(1)	3.182		0.15
R19	(i,j,k) (i,j,k)	Cl(2) · · O(2)	3.365		0.09
R20	(i,j,k) $(i,j,k-1)$	Cl(2) · · O(2)	3.445		0.07
R21	(i,j,k) $(i+1,j,k+1)$	Cl(2) · · O(2)	3.238		0.13
R22	(i,j,k) $(i+1,j,k+1)$	H(1) · · Cl(2)	2.236		0.15
R23	(i,j,k) (i,j,k)	H(2) · · Cl(2)	2.172		0.15
R24	(i,j,k) $(i-1,j,k)$	H(3) · · Cl(1)	2.222		0.15
R25	(i,j,k) $(i+1,j,k+1)$	H(4) · · Cl(1)	2.601		0.10
R26	(i,j,k) $(i+1,j,k+1)$	H(4) · · Cl(2)	2.492		0.10
R27	(i,j,k) (i,j,k)	H(1)—O(1)	0.967		5.83
R28	(i,j,k) $(i,j,k-1)$	H(2)—O(1)	0.974		5.83
R29	(i,j,k) (i,j,k)	H(3)—O(2)	0.965		5.83
R30	(i,j,k) (i,j,k)	H(4)—O(2)	0.953		5.83
R31	$(i,j,k+1)$ (i,j,k) (i,j,k)	Ba—O(1)—Ba	2.841	2.851	0.04
R32	(i,j,k) (i,j,k) (i,j,k)	Ba—O(2)—Ba	2.865	2.894	0.04
R33	(i,j,k) (i,j,k) $(i,j,k+1)$	H(1)—O(1)—H(2)	0.967	0.974	0.75
R34	(i,j,k) (i,j,k) (i,j,k)	H(3)—O(2)—H(4)	0.965	0.953	0.75
R35	$(i,j,k+1)$ (i,j,k) (i,j,k)	Ba—O(1)—H(1)	2.841	0.967	0.038
R36	$(i,j,k+1)$ (i,j,k) $(i,j,k+1)$	Ba—O(1)—H(2)	2.841	0.974	0.03
R37	(i,j,k) (i,j,k) (i,j,k)	Ba—O(1)—H(1)	2.851	0.967	0.038
R38	(i,j,k) (i,j,k) $(i,j,k+1)$	Ba—O(1)—H(2)	2.851	0.974	0.03
R39	(i,j,k) (i,j,k) (i,j,k)	Ba—O(2)—H(3)	2.865	0.965	0.03
R40	(i,j,k) (i,j,k) (i,j,k)	Ba—O(2)—H(4)	2.865	0.953	0.025
R41	(i,j,k) (i,j,k)	Ba—O(2)—H(3)	2.894	0.965	0.03
R42	(i,j,k) (i,j,k) (i,j,k)	Ba—O(2)—H(4)	2.894	0.953	0.025

Onec B_{opt}^{I} corresponding to the first molecular unit, *I*, is constructed, B_{opt} corresponding to the other molecular units can be obtained by symmetry operations. For BCD, for example, it is

$$B_{opt}^{II}=R_2B_{opt}^{I};\ B_{opt}^{III}=R_3B_{opt}^{I}$$

and $B_{opt}^{IV}=R_4B_{opt}^{I}$.

F_{opt} is diagonal in internal coordinates, if the potential energy can be set up without cross terms between any two internal coordinates.

One can obtain the lattice frequencies and their eigenvectors representation by transforming $G_{(c)}$ and $F_{(c)}$ (from here we drop the subscript 'opt', but it is always implied) using the relation,

$$G^{s}_{(c)}=UG_{(c)}\tilde{U} \tag{16}$$

$$F^{s}_{(c)}=UF_{(c)}\tilde{U} \tag{17}$$

where $\tilde{U}$ indicates the conjugate transposed symmetry adopted eigenvector matrix derived by the group-theoretical approach. To summarize, diagonalization of $G^{s}_{(c)}\cdot F^{s}_{(c)}$ results in obtaining the frequencies of optical vibrations of a crystalline lattice. The dimension of various matrices are $G_{(c)}$: $3n\times3n$, F: $NR\times NR$, B_{opt}: $NR\times3n$ and U: $3n\times3n$. *NR* is the number of interactions.

The potential energy of the crystal is assumed to be made up of two parts,

$$U=U_{H_2O}+U_{inter} \tag{18}$$

where U_{H_2O} is the Urey-Bradley force field associated with the crystal H_2O molecules, and U_{inter} represents the interaction potential between crystal water molecules and ions, between ions, and also between water molecules. For SBD, U_{inter} is assumed to be

$$\begin{aligned}2U_{inter}=\sum\{&f_{i\,Na-O}\Delta R^2_{i\,Na-O}\\&+f_{i\,Br-O}\Delta R^2_{i\,Br-O}+f_{i\,Na\cdots Na}\Delta R^2_{i\,Na\cdots Na}\\&+f_{i\,Na-Br}\Delta R^2_{i\,Na-Br}+f_{i\,H-Br}\Delta R^2_{i\,H-Br}\\&+H_{i\,Na-O-Na}r^2_{i\,Na-O}\Delta\alpha^2_{i\,Na-O-Na}\\&+H_{i\,Na-O-H}r_{i\,Na-O}r_{i\,H-O}\Delta\alpha^2_{i\,Na-O-H}\}\end{aligned} \tag{19}$$

by neglecting some trivial interactions and, similarly for BCD

$$\begin{aligned}2U_{inter}=\sum\{&f_{i\,C\bar{l}-H}\Delta R^2_{i\,C\bar{l}-H}\\&+f_{i\,Ba^{2+}-O}\Delta R^2_{i\,Ba^{2+}-O}\\&+f_{i\,Ba^{2+}-C\bar{l}}\Delta R^2_{i\,Ba^{2+}-C\bar{l}}+f_{i\,O-O}\Delta R^2_{i\,O-O}\\&+f_{i\,O-C\bar{l}}\Delta R^2_{i\,O-C\bar{l}}+f_{i\,C\bar{l}-C\bar{l}}\Delta R^2_{i\,C\bar{l}-C\bar{l}}\\&+H_{i\,H-O-Ba^{2+}}r_{i\,O-H}r_{i\,Ba^{2+}-O}\Delta\alpha^2_{i\,H-O-Ba^{2+}}\\&+H_{i\,Ba^{2+}-O-Ba^{2+}}r^2_{i\,Ba^{2+}-O}\Delta\alpha^2_{i\,Ba^{2+}-O-Ba^{2+}}\}\end{aligned} \tag{20}$$

In the above equations, the ΔR_i'*s* and $\Delta\alpha_i$'*s* represent interatomic displacements in distances and in bond angles respectively and the *r*'*s* represent equilibrium interatomic distances.

We have written a software for calculating the eigenfunctions and eigenvectors given G_c, F^t, B_{opt} and U matrices. The interactions with interatomic distances of more than 4Å(3.8Å in the case of BCD) have been neglected in Eqs. (19) and (20) and those interactions taken into account are shown for the first respective molecular unit in Tables 8 and 9 along with force constants adopted. The force constants in U_{H_2O} have been taken from Ref. (27) and the stretching force constants associated with non-bond pairs have been determined from the second derivatives of the electrostatic potentials at equilibrium interatomic distances using the point charges assigned in Table 2. Similarly the f_i(H···Y)'*s* have been determined from the second derivatives of U(H···Y), and H_i(O—H···M)'*s*, *M* being the metal ion, have been adjusted so as to obtain reasonable agreement of the calculated librational frequencies with observed frequencies. The results for A_u species are given in Table 10 along with the observed frequencies. It is seen that all of the calculated frequencies other than those from H_2O internal modes are due to highly mixed modes as expected from the discussion in 5-(ii). Therefore, only those modes identified as significant H_2O librational modes from their large potential energy. distribution in A_u species are assigned to the frequencies. The results from A_g, B_u, and B_g

Table 10. Comparison of the observed H_2O librational frequencies with the theoretical values (in cm^{-1}).

$NaBr \cdot 2H_2O$

Experimental		Theoretical		
IR[14]	Neutron (100°K)	GF method	Simple model	
			Total P.E.	H-bond P.E.
	650±8	658 W(2) R(2)	660 W(2)	
625		614 T(2) W(2)		
590		590 R(1) W(1)		599 T(2)
	562±6	558 R(1) T(1)	523 W(1)	566 R(2)
			519 R(1)	539 W(2)
470	474	478 R(2)	473 T(2)	440 W(1)
405	403±5	393 R(1) T(1)	385 T(1)	389 R(1)
				366 T(1)

$BaCl_2 \cdot 2H_2O$

Experimental				Theoretical		
IR[15]	Raman[15]	T-O-F[1] (300°K)	Neutoron (100°K)	GF method	Simple model	
					Tabal P.E.	H-bond P.E.
715	714	660±40	717±15	740 R(2) W(2)	751 W(1)	
686				651 W(1)	646 W(2)	638 R(1)
						635 T(1)
592	611		601±9	585 T(1)	619 R(1)	596 W(1)
					600 T(1)	
561		536±32	568(?)			
536	490	480±24	531	539 R(2) T(2)		477 W(2)
420	407	384±16	423±5	420 R(2) W(2)	425 T(2)	432 R(2)
411						
330				360 R(1)	308 R(2)	359 T(2)

species are almost same as A_u species as far as the H_2O librations are concerned. Similar calculation was also carried out for BCD earlier by Fukushima et al[27]. Due to some differences in adopting relevant force constants, there is no detailed agreement between two works.

As already pointed out, the shapes of the librational potential energy curves based on the simple model can not represent the structure data satisfactorily for the H_2O molecule involved either in highly bent or bifurcated H-bond. In fact, the possibility of extending LSPF to these H-bond configurations remains to be studied in further detai. As can be seen in Table 10, however, the agreement between experimental and theoretical frequencies obtained from FG method may be considered fair with all simplification of estimating the non-linear H-bond interactions. This might be partly due to the parametrization of H_i(O-H···M)'s.

As mentioned earlier, both methods, neutron and optical, do not observe exactly the same one. Without either detailed coherent neutron inelastic scattering measurements or calcuation of complete lattice dynamics, it is difficult to say whether the disagreements in the observed frequencies by neutron and optical method are due to the dispersion of the librational branches or difference in the selection rule of both methods. Although neutorn method is free from selection rules, some peaks may not be seen because of unfavorable polarization conditions. Considering theses facts it is interesting to note that the observations from neutron and optical methods

hold agreements complementally to the theoretical frequencies obtained from FG method in both samples.

It is remarkable that the H_2O librational frequencies are found to be more sensitive to H_i(H-O···M)'s, namely bending interactions between the metal ions and the lone pair orbitals of O atoms, than f_i(H···Y)'s in FG method in contrast to the dominant contribution of H-bond in the simple model. This may be due to ignoring of O-H···Y bendings in Eqs. (19) and (20). In other words, the H-bond interacton based on U(H···Y) is the pure central force field and accordingly produces less bending component on the non-rigid H_2O librators, compared with the case of simple model. In the absence of reliable H_i(H-O···M)'s we think that it does not provide much informations to include H_i(O-H···Y)'s terms in Eqs. (19) and (20) and parametrize the values in the framework of the present approach. However, in view of the fact that the frequencies from the H-bond interaction alone are able to predict roughly the magnitude of the observed values in the simple model, the above discussion may be led to that the effect of O-H···Y bending interactions are merged implicitly in H_i(H-O···M)'s parametrized in FG method. Further detailed study of this problem in various crystal hydrates, will provide more understanding of the nature of H-bonds and the role of metal-oxygen coordinations in H_2O librations.

Acknowledements

The authors are greatly indebted to. Dr. K. R. Rao for many valuable discussions and detailed comments on theoretical treatments. Acknowledgments are also made to Drs. R. A. Chidambaram and S. K. Sikka for useful discussions on hydrogen bond interaction and calculation of crystal energy. We also wish to thank Dr. Moon Kyu Chung and Dr. Hae-Ill Bak for their constant interest and encouragement throughout this work.

Thanks are also due to Mr. Han-Giu Kim who had joined to this work at the stage of construction of the inverted filter spectrometer. Valuble technical assistanc has been provided by Mr. Byung Chil Chun.

References

1. H. Boutin et al., J. Chem. Phys. **40**, 2670 (1974); H. Prask and H. Boutin, J. Chem. Phys. **45**, 699 (1966); **45**, 1685 (1966)
2. A. Bajorek et al., Neutron Inelastic Scattering, **2**, 143, IAEA, Vienna (1968)
3. C. L. Taper et al., Phys. Stat. Sol. **34**, 279 (1969)
4. C. L. Taper et al., Solid State Comm. **7**, 496 (1970)
5. K. Ichida et al., Spectrochimica 28A, 2433 (1972)
6. R. Chidambaram, A. Sequeiria and S. K. Sikka, J. Chem. Phys. **41**, 3616 (1964)
7. J. P. Culot, P. Piret & M. V. Meerssche, Bull. Soc. Franc. Miner. Crist. **85**, 282 (1962); **85**, 290 (1962); M. F. C. Ladd, Z. Krist. **126**, 147 (1968)
8. V. M. Podmanabhan, W. R. Busing and H. A. Levy, Acta Cryst. **16** A26 (1963); W. H. Baur, Acta Cryst. **19**, 909 (1965)
9. Woods, A. D. B., Brockhouse, B. N., Sakameto, M. and Sinclair, R. N., Inelastic Scattering of Neutrons in Solids and Liquids, IAEA, Vienna, 487 (1961)
10. H. J. Kim H. K, Kim and B. G. Yoon, in the AERI Proceeding of a Study Group Meeting on Research Reactor Utilization, IAEA-147, 301, (1972) The design, construction and our experiences on the improvement of the perfaomance of the inverted filter spectrometer will be published seperately.
11. J. S. Sarma, J. Chem. Phys. **52**, 377 (1970)
12. H. J. Kim, P. S. Goyal, G. Venkataraman, B. A. Dasanncharya and C. L. Taper Solid State

Comm. **8**, 889 (1970)
13. H. J. Kim, J. Kor. Nucl. Soc., **4**, 306 (1972)
14. J. Van der Elsken and D. W. Robinson, Spectrochim, Acta **17**, 1249 (1961)
15. Y. S. Jain, V. K. Kapoor and H. D. Dist, Appl. Spectroscopy **30**, 440 (1976)
16. H. Hahn, Inelastic Scattering of Neutron Scattering, IAEA, Vienna, **2**, 279 (1965); H. Prask, H. Boutin and S. Yip, J. Chem. Phys. **48**, 3367 (1968)
17. Y. S. Jain, Solid State Comm. **17**, 650 (1975)
18. Thaper, C. L., Dasannacharya, B. A., Iyengar, P. K. and Srinivasan, T., B. A. R. C. Report BARC 501 **61** (1970)
19. A. Sfolander, Arkiv for Fysik **14**, 315 (1958)
20. E. R. Lippincott and R. Schroeder, J. Chem. Phys. **23**, 1099 (1955)
21. R. Chidambaram and S. K. Sikka, Chem. Phys. Letters, **2**, 162 (1968); R. Balasubramanian, R. Chidambaiam and G. N. Ramachandrau, Biochim. Biophys. Acta **221**, 182 (1970); **221**, 196 (1970)
22. A. I. Kitaigorodskii, Acta Cryst. B27, 868 (1971)
23. J. A. Pople, Proc. Roy. Soc. **202A**, 323 (1950)
24. A. A. Maradudin and S. H. Vosko, Rev. Mod. Phys. **40**, 1 (1968)
25. G. Venkataraman and V. C. Saųni, Rev. Mod. Phys. **42**, 409 (1970)
26. T. Shimanouchi, M. Tsubni and T. Miyazawa, J. Chem. Phys. **35**, 1597 (1961)
27. K. Fukushima and H. Kataiwa, Chem. Soc. Japan, **43**, 690 (1970)